



This is a repository copy of *Mono-scale and multi-scale formulations of gradient-enriched dynamic piezomagnetism*.

White Rose Research Online URL for this paper:  
<http://eprints.whiterose.ac.uk/150512/>

Version: Accepted Version

---

**Article:**

Xu, M., Askes, H. [orcid.org/0000-0002-4900-1376](https://orcid.org/0000-0002-4900-1376) and Gitman, I.M. (2019) Mono-scale and multi-scale formulations of gradient-enriched dynamic piezomagnetism. *Wave Motion*, 91. ISSN 0165-2125

<https://doi.org/10.1016/j.wavemoti.2019.102402>

---

Article available under the terms of the CC-BY-NC-ND licence  
(<https://creativecommons.org/licenses/by-nc-nd/4.0/>).

**Reuse**

This article is distributed under the terms of the Creative Commons Attribution-NonCommercial-NoDerivs (CC BY-NC-ND) licence. This licence only allows you to download this work and share it with others as long as you credit the authors, but you can't change the article in any way or use it commercially. More information and the full terms of the licence here: <https://creativecommons.org/licenses/>

**Takedown**

If you consider content in White Rose Research Online to be in breach of UK law, please notify us by emailing [eprints@whiterose.ac.uk](mailto:eprints@whiterose.ac.uk) including the URL of the record and the reason for the withdrawal request.



[eprints@whiterose.ac.uk](mailto:eprints@whiterose.ac.uk)  
<https://eprints.whiterose.ac.uk/>

# Mono-scale and multi-scale formulations of gradient-enriched dynamic piezomagnetism

Mingxiu Xu<sup>a</sup>, Harm Askes<sup>b</sup>, Inna M. Gitman<sup>c,\*</sup>

<sup>a</sup>*Department of Applied Mechanics, School of Mathematics and Physics,  
University of Science and Technology Beijing, China*

<sup>b</sup>*Department of Civil and Structural Engineering, The University of Sheffield, UK*

<sup>c</sup>*Department of Mechanical Engineering, The University of Sheffield, UK*

---

## Abstract

In this contribution, we combine and extend earlier work on static piezomagnetism and dynamic gradient elasticity to develop novel dynamic piezomagnetic continuum models. The governing equations can be formulated as a mono-scale model or as multi-scale models. The latter include full coupling between micro and macro-scale displacements and micro and macro-scale magnetic potentials, which allows to denote these as “multi-scale multi-physics” models. The field equations and boundary conditions are given together with the underlying energy functionals. An analysis of coupled dispersive waves is carried out to illustrate the behaviour of the models and their ability to simulate dispersive piezomagnetic waves.

*Keywords:* piezomagnetism, generalised continuum, multi-scale, multi-physics, length scale, wave dispersion

---

## 1. Introduction

With increasing levels of miniaturisation of structures and systems, the underlying microstructures of materials become more and more relevant. They need to be accounted for in modelling approaches for accurate and reliable descriptions and predictions of the physical behaviour of these structures and systems. Using continuum theories is a popular modelling methodology, however, in the absence of terms representing the microstructure, classical continuum theory cannot describe the mechanical or physical behaviour of materials at the micro or

---

\*Corresponding Author: [i.gitman@sheffield.ac.uk](mailto:i.gitman@sheffield.ac.uk)

nano scale and capture the size effects observed experimentally—see for instance [1, 2, 3] for typical studies. Similarly, in dynamic problems classical continuum theory cannot describe dispersive wave propagation [4, 5]. This is particularly inadequate when the wavelength of an incident wave is comparable to the length of the material microstructure [6, 7].

It has been shown on many occasions that the inclusion of higher-order spatial derivatives of one or more relevant state variables can address the shortcomings mentioned above. Such higher-order gradient terms permit the prediction of size-dependent response as well as dispersive wave propagation, and indeed the length scale parameters that accompany these higher-order gradients can typically be linked to microstructural properties. Thus, gradient-enriched elasticity theories have been used successfully to analyse a range of phenomena including buckling, vibration and wave propagation [8, 9, 10, 11, 12, 13]. Furthermore, new gradient-enriched elasticity models, such as complete anisotropic strain-gradient elasticity [14, 15], spatial-temporal nonlocal homogenisation models [16, 17] and dispersive gradient elasticity with multiple micro-inertia terms [18, 19], have increased the versatility of the gradient elasticity modelling framework. In parallel, procedures for the identification of model coefficients, including higher-order length scales, have been presented in [20, 21, 22]. An overview of formulations and length scale identification procedures can be found in [23].

In dynamic magneto-mechanical coupling, Mindlin’s gradient theory [24] has been used in the vibration analysis of micro-bar and nano-plates [25]. Similarly, Eringen’s gradient theory [26] has been employed to analyse the effects of magnetic field on the vibration of [27, 28, 29], and wave propagation in [30, 31], carbon nanotubes and nano-beams. A Kelvin–Voigt model [32] has been used to explore the effect of magnetic field on the vibration of graphene sheet with different Winkler coefficients [33]. Nonlocal strain gradient theory has been employed to analyse the effect of magnetic field on wave propagation in viscoelastic single-walled carbon nanotubes [34]. However, in these applications, the length scales included in the model appear in the mechanical equations only, and the influence of microstructure on the magnetic properties is not accounted for—whereas the magnetic parameters have also been shown to be influenced by the microstructure of the material [35]. Therefore, for a more versatile description of coupled mechanical-magnetic behaviour, it seems pertinent to include microstructural terms in both the mechanical equations and the magnetic equations.

Considering gradients in the stress, electric displacement and magnetic induction by introducing one scale parameter, magneto-electro-elastic coupling has been analysed based on Eringen’s nonlocal theory [36, 37, 38]. Furthermore, an

additional scale parameter can be added to account for gradients in the conjugated variables of strain, electric field and magnetic field, again based on Eringen's theory [39, 40, 41, 42, 43]. However, in the referred studies the three coupled physical fields are all equipped with the same length scale. Different length scales for different physical fields have been considered in electro-mechanical coupling [44] and magneto-mechanical coupling [45]. In this paper we will expand the latter study towards dynamics. In particular, we will explore multi-scale formulations of dynamic piezo-magnetic coupling, whereby micro and macro scale displacements and magnetic potentials are all included explicitly in the model. Not only has this the advantage of being able to distinguish clearly between the two scales, it also facilitates potential finite element implementations [23]. This study has an explorative character and is restricted to one-dimensional models, but extension to multiple dimensions is straightforward.

## 2. Extending the static piezomagnetism model to dynamics

Building on the earlier work of Aifantis and coworkers [44], we presented a gradient-enriched static piezomagnetic model in [45], the one-dimensional version of which reads

$$E (u'' - \ell_1^2 u'''' ) + q (\varphi'' - \ell_2^2 \varphi'''' ) = 0 \quad (1a)$$

$$-q (u'' - \ell_2^2 u'''' ) + \mu (\varphi'' - \ell_3^2 \varphi'''' ) = 0 \quad (1b)$$

where dashes denote spatial derivatives. Furthermore,  $E$  is the Young's modulus,  $\mu$  is the magnetic permeability and  $q$  is the piezo-magnetic coupling constant. In addition to the three standard piezomagnetic terms, the model also contains three higher-order terms accompanied with length-scale parameters  $\ell_1$ ,  $\ell_2$  and  $\ell_3$ . The primary scalar unknowns are the displacement  $u$  and the magnetic potential  $\varphi$ . In the multi-dimensional format given in [45], the displacement is a vectorial quantity and the magnetic potential is a scalar. The underlying assumptions are that the density of free charge is zero, and that the medium is transparent and insulated. Therefore, the electric field does not act as a source field and a scalar magnetic potential  $\varphi$  can be introduced, according to Maxwell's equations, to describe the magnetic field  $H = -\nabla\varphi$  such that  $\nabla \times H = 0$ .

In [45] we showed that the higher-order mechanical term related to  $\ell_1$  is essential to remove singularities from the strain field and to capture size-dependent behaviour of the mechanical fields. Similarly, the higher-order magnetic term related to  $\ell_3$  is required to remove singularities from the magnetic field and to

capture size-dependent behaviour of the magnetic field variables. Conversely, the higher-order coupling term related to  $\ell_2$  was shown to be of quantitative importance only—and in this context it is noted that Aifantis and coworkers left out the higher-order coupling term proportional to  $\ell_2$  [44].

Whereas the main motivations for gradient enrichment in statics are the removal of singularities and the ability to describe size-dependent response, an additional motivation for gradient enrichment in dynamics is the ability to describe dispersive wave propagation. It is well-known that the higher-order terms included in Eqns. (1) are not suitable for this purpose, as they lead to unbounded phase velocities. Instead, the desired effect can be obtained by enriching the **transient terms** with bespoke higher-order gradient contributions. This leads to

$$E(u'' - \ell_1^2 u''''') + q(\varphi'' - \ell_2^2 \varphi''''') = \rho(\ddot{u} - \ell_4^2 \ddot{u}'') \quad (2a)$$

$$-q(u'' - \ell_2^2 u''''') + \mu(\varphi'' - \ell_3^2 \varphi''''') = \mu^2 e(\ddot{\varphi} - \ell_5^2 \ddot{\varphi}'') \quad (2b)$$

where superimposed dots denote time derivatives. Furthermore,  $\rho$  is the mass density,  $e$  is the electric permittivity, and  $\ell_4$  and  $\ell_5$  denote two additional length scale parameters. The Lagrangian density  $\mathcal{L}$  associated with Eqns. (2) can be written as

$$\mathcal{L} = \mathcal{L}_{\text{elastic}} + \mathcal{L}_{\text{coupling}} - \mathcal{L}_{\text{magnetic}} \quad (3)$$

with

$$\mathcal{L}_{\text{elastic}} = \frac{1}{2}\rho \left\{ (\dot{u})^2 + \ell_4^2 (\dot{u}')^2 \right\} - \frac{1}{2}E \left\{ (u')^2 + \ell_1^2 (u'')^2 \right\} \quad (4a)$$

$$\mathcal{L}_{\text{coupling}} = -q \left\{ u' \varphi' + \ell_2^2 u'' \varphi'' \right\} \quad (4b)$$

$$\mathcal{L}_{\text{magnetic}} = \frac{1}{2}\mu^2 e \left\{ (\dot{\varphi})^2 + \ell_5^2 (\dot{\varphi}')^2 \right\} - \frac{1}{2}\mu \left\{ (\varphi')^2 + \ell_3^2 (\varphi'')^2 \right\} \quad (4c)$$

Evidently, the model of Eqns. (2) and (4) is “multi-physics”, but the primary unknowns  $u$  and  $\varphi$  are defined as mono-scale variables. It may be of interest to reformulate the equations so as to be able to identify micro-scale and macro-scale effects separately. In addition, it may equally be of interest to reduce the highest order of spatial derivation from four to two, which greatly facilitates finite element implementations. In the next Section, it will be shown that both goals can be achieved simultaneously.

**Remark 1.** *In our earlier work in statics, we explored piezomagnetic formulations with either  $\varphi$  or  $H = -\nabla\varphi$  as the magnetic primary unknown [45]. However,*

*in the dynamic context of this paper we wish to maintain symmetry of the resulting equations. It has turned out to be necessary to use  $\varphi$  as the magnetic primary unknown, which constrains the format of the variationally consistent boundary conditions. To mimic essential boundary conditions in terms of  $H$ , we suggest to use natural boundary conditions in terms of  $\varphi$ .*

### 3. Multi-scale dynamic piezomagnetic models

The dynamic gradient elasticity model associated with Eq. (4a) was reformulated in [46, 47] by distinguishing between micro-scale displacements  $u_m$  and macro-scale displacements  $u_M$ . This is based on the equivalence of integral relations used in homogenisation theory and differential relations used in gradient theory. Starting point is the definition of a macro-scale variable (e.g. the displacement) as the volume average over a Representative Volume Element  $\Omega_{\text{RVE}}$  of the equivalent micro-scale variable

$$u_M \equiv \frac{1}{\Omega_{\text{RVE}}} \int_{\Omega_{\text{RVE}}} u_m \, dV \quad (5a)$$

Next,  $u_m$  may be developed in a Taylor series around its value at the centre of  $\Omega_{\text{RVE}}$ . The integrals can then be elaborated, resulting in

$$u_M = u_m + \ell^2 \nabla^2 u_m + \dots \quad (5b)$$

where  $\ell$  is a representative dimension of the Representative Volume Element. Using Padé approximations [6], the series of Eq. (5b) can be translated into

$$u_M - \ell^2 \nabla^2 u_M + \dots = u_m \quad (5c)$$

which is equivalent to Eq. (5b) and therefore also to Eq. (5a).

Using the second-order truncation of Eq. (5c) in one spatial dimension, and identifying the displacement variable in Eq. (1) as the macro-scale displacement, second-order derivatives of the macro-scale displacement can be replaced by the difference between macro-scale and micro-scale displacement. After some algebra, a new Lagrangian density  $\mathcal{L}_{\text{elastic}}$  was found [46, 47] as a replacement of Eq. (4a):

$$\mathcal{L}_{\text{elastic}} = \frac{1}{2} \rho \left\{ (\dot{u}_m)^2 + \frac{\ell_4^2 - \ell_1^2}{\ell_1^2} (\dot{u}_m - \dot{u}_M)^2 + (\ell_4^2 - \ell_1^2) (\dot{u}'_M)^2 \right\} - \frac{1}{2} E (u'_m)^2 \quad (6)$$

Note that in Eq. (6) all gradient-enrichment is included in the kinetic energy terms, rather than in the strain energy terms. This methodology will next be extended to dynamic piezomagnetism for two specific modelling particularisations.

### 3.1. Multi-scale model 1: ignoring *transient magnetic effects*

It is well-known that the wave speeds of elastic waves and of magnetic waves differ by several orders of magnitude. When concentrating on the elastic waves, one could thus argue that magnetic effects happen virtually instantaneously and that there is a clear separation of time scales. This motivates a simplification of Eq. (2b) in ignoring the right-hand-side. If furthermore the assumption  $\ell_3 = \ell_2 = \ell_1$  is made, Eqns. (2) can be written as

$$Eu_m'' + q\varphi_m'' = \rho (\ddot{u}_M - \ell_4^2 \ddot{u}_M'') \quad (7a)$$

$$-qu_m'' + \mu\varphi_m'' = 0 \quad (7b)$$

where, following Eq. (5),  $u_m = u_M - \ell_1^2 u_M''$  and  $\varphi_m = \varphi_M - \ell_1^2 \varphi_M''$ . A symmetric formulation can be obtained by taking the acceleration format of the former, that is  $\dot{u}_m = \dot{u}_M - \ell_1^2 \dot{u}_M''$ , by which the last term in Eq. (7a) can be rewritten. This gives the following set of coupled equations:

$$Eu_m'' + q\varphi_m'' = \rho \left( \frac{\ell_4^2}{\ell_1^2} \ddot{u}_m - \frac{\ell_4^2 - \ell_1^2}{\ell_1^2} \ddot{u}_M \right) \quad (8a)$$

$$0 = \rho \frac{\ell_4^2 - \ell_1^2}{\ell_1^2} (-\ddot{u}_m + \ddot{u}_M - \ell_1^2 \ddot{u}_M'') \quad (8b)$$

$$-qu_m'' + \mu\varphi_m'' = 0 \quad (8c)$$

$$-\varphi_m + \varphi_M - \ell_1^2 \varphi_M'' = 0 \quad (8d)$$

Eqns. (8a–8c) form a fully coupled, symmetric system of equations with unknowns  $u_m$ ,  $u_M$  and  $\varphi_m$ , the Lagrangian density of which reads

$$\begin{aligned} \mathcal{L} = & \frac{1}{2}\rho \left\{ (\dot{u}_m)^2 + \frac{\ell_4^2 - \ell_1^2}{\ell_1^2} (\dot{u}_m - \dot{u}_M)^2 + (\ell_4^2 - \ell_1^2) (\dot{u}_M')^2 \right\} \\ & - \frac{1}{2}E (u_m')^2 - qu_m' \varphi_m' + \frac{1}{2}\mu (\varphi_m')^2 \end{aligned} \quad (9)$$

Note that  $\varphi_M$  does not appear in Eqns. (8a–8c); thus, Eq. (8d) is decoupled from Eqns. (8a–8c) and can be solved as a post-processing step once  $\varphi_m$  is found.

**Remark 2.** *The boundary conditions associated with Eqns. (8a–8c) turn out to be the same as for the next model, and will thus not be treated separately—see Eqns. (17a–17c) below.*

### 3.2. Multi-scale model 2: including *transient magnetic effects*

On the other hand, for a more general description it may be required to **model finite magnetic response times by including transient magnetic terms, cf. the right-hand-side of Eq. (2b)**. A multi-scale formulation may then be obtained **by postulating a Lagrangian density associated with the magnetic response that has the same structure as the Lagrangian density associated with the elastic response**. Thus, similar to replacing Eq. (4a) with Eq. (6), we will replace Eq. (4c) with

$$\begin{aligned} \mathcal{L}_{\text{magnetic}} = & \frac{1}{2} \mu^2 e \left\{ (\dot{\phi}_m)^2 + \frac{\ell_5^2 - \ell_3^2}{\ell_3^2} (\dot{\phi}_m - \dot{\phi}_M)^2 + (\ell_5^2 - \ell_3^2) (\dot{\phi}'_M)^2 \right\} \\ & - \frac{1}{2} \mu (\phi'_m)^2 \end{aligned} \quad (10)$$

In addition, following Eq. (9), we write the Lagrangian density of the piezomagnetic coupling in terms of the micro-scale quantities:

$$\mathcal{L}_{\text{coupling}} = -q u'_m \phi'_m \quad (11)$$

Note that  $\ell_2$  is absent from this formulation. Substituting Eqns. (6), (10) and (11) into Eq. (3), **standard variational principles can be used to derive the field equations and boundary conditions. We require**

$$\delta \int_0^X \int_0^T \mathcal{L} dt dx = \int_0^X \int_0^T \delta \mathcal{L} dt dx = 0 \quad (12)$$

where the integrations in space and time are carried out over intervals  $0 \leq x \leq X$  and  $0 \leq t \leq T$ , respectively. Noting that

$$\mathcal{L} = \mathcal{L} (u'_m; \dot{u}_m; \dot{u}_M; \dot{u}'_M; \phi'_m; \dot{\phi}_m; \dot{\phi}_M; \dot{\phi}'_M) \quad (13)$$

we obtain

$$\begin{aligned} & \int_0^X \int_0^T \left( \delta u'_m \frac{\partial \mathcal{L}}{\partial u'_m} + \delta \dot{u}_m \frac{\partial \mathcal{L}}{\partial \dot{u}_m} + \delta \dot{u}_M \frac{\partial \mathcal{L}}{\partial \dot{u}_M} + \delta \dot{u}'_M \frac{\partial \mathcal{L}}{\partial \dot{u}'_M} \right) dt dx + \\ & \int_0^X \int_0^T \left( \delta \phi'_m \frac{\partial \mathcal{L}}{\partial \phi'_m} + \delta \dot{\phi}_m \frac{\partial \mathcal{L}}{\partial \dot{\phi}_m} + \delta \dot{\phi}_M \frac{\partial \mathcal{L}}{\partial \dot{\phi}_M} + \delta \dot{\phi}'_M \frac{\partial \mathcal{L}}{\partial \dot{\phi}'_M} \right) dt dx = 0 \end{aligned} \quad (14)$$

Carrying out integration by parts results in

$$\begin{aligned}
& \int_0^X \int_0^T \delta u_m \left( -\frac{\partial}{\partial x} \frac{\partial \mathcal{L}}{\partial u'_m} - \frac{\partial}{\partial t} \frac{\partial \mathcal{L}}{\partial \dot{u}_m} \right) dt dx + \int_0^T \left[ \delta u_m \frac{\partial \mathcal{L}}{\partial u'_m} \right]_0^X dt + \\
& \int_0^X \left[ \delta u_m \frac{\partial \mathcal{L}}{\partial \dot{u}_m} \right]_0^T dx + \int_0^X \int_0^T \delta u_M \left( -\frac{\partial}{\partial t} \frac{\partial \mathcal{L}}{\partial \dot{u}_M} + \frac{\partial^2}{\partial t \partial x} \frac{\partial \mathcal{L}}{\partial \dot{u}'_M} \right) dt dx + \\
& \int_0^X \left[ \delta u_M \frac{\partial \mathcal{L}}{\partial \dot{u}_M} \right]_0^T dx + \int_0^X \left[ \delta u'_M \frac{\partial \mathcal{L}}{\partial \dot{u}_M} \right]_0^T dx - \int_0^T \left[ \delta u_M \frac{\partial}{\partial t} \frac{\partial \mathcal{L}}{\partial \dot{u}'_M} \right]_0^X dt + \\
& \int_0^X \int_0^T \delta \varphi_m \left( -\frac{\partial}{\partial x} \frac{\partial \mathcal{L}}{\partial \varphi'_m} - \frac{\partial}{\partial t} \frac{\partial \mathcal{L}}{\partial \dot{\varphi}_m} \right) dt dx + \int_0^T \left[ \delta \varphi_m \frac{\partial \mathcal{L}}{\partial \varphi'_m} \right]_0^X dt + \\
& \int_0^X \left[ \delta \varphi_m \frac{\partial \mathcal{L}}{\partial \dot{\varphi}_m} \right]_0^T dx + \int_0^X \int_0^T \delta \varphi_M \left( -\frac{\partial}{\partial t} \frac{\partial \mathcal{L}}{\partial \dot{\varphi}_M} + \frac{\partial^2}{\partial t \partial x} \frac{\partial \mathcal{L}}{\partial \dot{\varphi}'_M} \right) dt dx + \\
& \int_0^X \left[ \delta \varphi_M \frac{\partial \mathcal{L}}{\partial \dot{\varphi}_M} \right]_0^T dx + \int_0^X \left[ \delta \varphi'_M \frac{\partial \mathcal{L}}{\partial \dot{\varphi}_M} \right]_0^T dx - \int_0^T \left[ \delta \varphi_M \frac{\partial}{\partial t} \frac{\partial \mathcal{L}}{\partial \dot{\varphi}'_M} \right]_0^X dt = 0 \quad (15)
\end{aligned}$$

The terms that contain spatial integration and evaluations at times  $t = 0$  and  $t = T$  can be assumed to vanish identically, following standard arguments. The remaining integrals are required to vanish individually and thus lead to the following field equations:

$$\rho \frac{\ell_4^2}{\ell_1^2} \ddot{u}_m - \rho \frac{\ell_4^2 - \ell_1^2}{\ell_1^2} \ddot{u}_M - E u''_m - q \varphi''_m = 0 \quad (16a)$$

$$\rho \frac{\ell_4^2 - \ell_1^2}{\ell_1^2} (\ddot{u}_M - \ddot{u}_m) - \rho (\ell_4^2 - \ell_1^2) \ddot{u}''_M = 0 \quad (16b)$$

$$\mu^2 e \frac{\ell_5^2}{\ell_3^2} \ddot{\varphi}_m - \mu^2 e \frac{\ell_5^2 - \ell_3^2}{\ell_3^2} \ddot{\varphi}_M + q u''_m - \mu \varphi''_m = 0 \quad (16c)$$

$$\mu^2 e \frac{\ell_5^2 - \ell_3^2}{\ell_3^2} (\ddot{\varphi}_M - \ddot{\varphi}_m) - \mu^2 e (\ell_5^2 - \ell_3^2) \ddot{\varphi}''_M = 0 \quad (16d)$$

Eqns. (16b) and (16d) provide the multi-scale coupling in the spirit of Eq. (5), provided  $\ell_4 \neq \ell_1$  and  $\ell_5 \neq \ell_3$ .

Eq. (15) also yields the following boundary conditions:

$$\text{either prescribe } u_m \quad \text{or prescribe } Eu'_m + q\phi'_m \equiv \sigma \quad (17a)$$

$$\text{either prescribe } u_M \quad \text{or prescribe } \rho (\ell_4^2 - \ell_1^2) \dot{u}'_M \quad (17b)$$

$$\text{either prescribe } \phi_m \quad \text{or prescribe } qu'_m - \mu \phi'_m \equiv B \quad (17c)$$

$$\text{either prescribe } \phi_M \quad \text{or prescribe } \mu^2 e (\ell_5^2 - \ell_3^2) \dot{\phi}'_M \quad (17d)$$

Note that expressions (17a) and (17c) include the standard definitions of the stress  $\sigma$  and the magnetisation flux density  $B$ .

#### 4. Dispersion analysis

The behaviour of the models is compared through an analysis of dispersive waves. An infinitely long medium is assumed, and simultaneous perturbations of the various coupled fields are assumed with phase velocity  $c$  and wave number  $k$ .

##### 4.1. Fourth-order mono-scale model

First, we investigate the original fourth-order mono-scale model. Ansatz functions  $u(x, t) = U \exp(ik(x - ct))$  and  $\phi(x, t) = \Phi \exp(ik(x - ct))$  are substituted into Eqns. (2), where  $U$  and  $\Phi$  are the amplitudes of the harmonic waves. This yields

$$E (1 + \ell_1^2 k^2) U + q (1 + \ell_2^2 k^2) \Phi = \rho c^2 (1 + \ell_4^2 k^2) U \quad (18a)$$

$$-q (1 + \ell_2^2 k^2) U + \mu (1 + \ell_3^2 k^2) \Phi = \mu^2 e c^2 (1 + \ell_5^2 k^2) \Phi \quad (18b)$$

Elimination of  $U$  and  $\Phi$  then leads to a quadratic equation in  $c^2$  as

$$\left( \frac{c^2}{c_m^2} \cdot \frac{1 + \ell_3^2 k^2}{1 + \ell_2^2 k^2} - 1 \right) \left( \frac{c^2}{c_e^2} \cdot \frac{1 + \ell_4^2 k^2}{1 + \ell_1^2 k^2} - 1 \right) + \frac{q^2}{\mu E} \cdot \frac{(1 + \ell_2^2 k^2)^2}{(1 + \ell_1^2 k^2)(1 + \ell_3^2 k^2)} = 0 \quad (19)$$

where  $c_m = 1/\sqrt{\mu e}$  and  $c_e = \sqrt{E/\rho}$  are the standard magnetic wave velocity and elastic wave velocity, respectively.

##### 4.2. Multi-scale model without *transient magnetic effects*

For the multi-scale model without transient magnetic effects, Eq. (8c) can be used to eliminate  $\phi_m''$  from Eq. (8a). Next, we substitute  $u_m(x, t) = U_m \exp(ik(x - ct))$  and  $u_M(x, t) = U_M \exp(ik(x - ct))$  into Eqns. (8a–8b), which gives

$$\left( E + \frac{q^2}{\mu} \right) U_m = \rho c^2 \left( \frac{\ell_4^2}{\ell_1^2} U_m - \frac{\ell_4^2 - \ell_1^2}{\ell_1^2} U_M \right) \quad (20a)$$

$$U_m = U_M (1 + \ell_1^2 k^2) \quad (20b)$$

Elimination of the two amplitudes  $U_m$  and  $U_M$  then yields straightforwardly

$$\frac{c^2}{c_e^2} \cdot \frac{1 + \ell_4^2 k^2}{1 + \ell_1^2 k^2} = 1 + \frac{q^2}{\mu E} \quad (21)$$

This is qualitatively similar to the results found in [48] for the multi-scale dynamic gradient elasticity model of Eq. (6), the only difference being the right-hand-side which can be considered to be a correction of the elastic wave velocity due to piezomagnetic coupling.

#### 4.3. Multi-scale model with *transient magnetic effects*

For the fully coupled model of Eqns. (16) four simultaneous perturbations are used, namely  $u_m(x, t) = U_m \exp(ik(x - ct))$  and  $u_M(x, t) = U_M \exp(ik(x - ct))$  for the two displacement fields, as well as  $\varphi_m(x, t) = \Phi_m \exp(ik(x - ct))$  and  $\varphi_M(x, t) = \Phi_M \exp(ik(x - ct))$  for the two magnetic potentials. Via expressions (16b) and (16d) the macro-scale amplitudes  $U_M$  and  $\Phi_M$  can be expressed in terms of their micro-scale equivalents  $U_m$  and  $\Phi_m$ . Equations (16a) and (16c) then yield

$$EU_m + q\Phi_m = \rho c^2 \frac{1 + \ell_4^2 k^2}{1 + \ell_1^2 k^2} U_m \quad (22a)$$

$$-qU_m + \mu\Phi_m = \mu^2 e c^2 \frac{1 + \ell_5^2 k^2}{1 + \ell_3^2 k^2} \Phi_m \quad (22b)$$

Elimination of the two remaining amplitudes results in a quadratic equation in terms of  $c^2$  as

$$\left( \frac{c^2}{c_m^2} \cdot \frac{1 + \ell_5^2 k^2}{1 + \ell_3^2 k^2} - 1 \right) \left( \frac{c^2}{c_e^2} \cdot \frac{1 + \ell_4^2 k^2}{1 + \ell_1^2 k^2} - 1 \right) + \frac{q^2}{\mu E} = 0 \quad (23)$$

which is identical to Eq. (19) except for the last term.

## 5. Results, comparisons and discussion

The response of the three models, i.e. the original mono-scale model and the two multi-scale models with and without *transient magnetic effects*, can be analysed and compared via the three dispersion relations of Eqns. (19), (21) and (23). Firstly, we will assume  $c_m \rightarrow \infty$ . It is straightforward to see that in this case Eq. (23) reduces to Eq. (21). If in addition we take  $\ell_3 = \ell_2 = \ell_1$ , also Eq. (19) becomes identical to Eq. (21); this is consistent with the assumptions made in deriving the

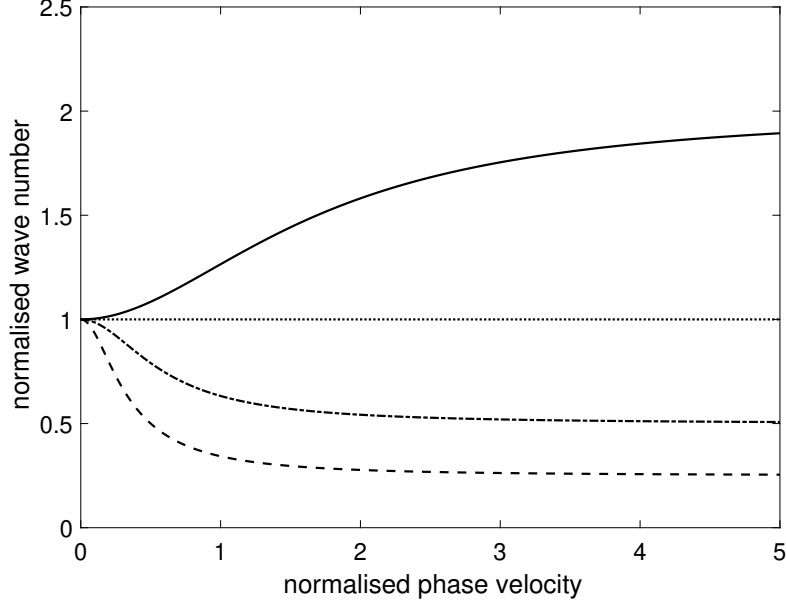


Figure 1: Normalised phase velocity  $c/c_e\sqrt{1+q^2/\mu E}$  against normalised wave number  $\ell_1 k$  for infinite  $c_m$ :  $\ell_4/\ell_1 = \frac{1}{2}$  (solid),  $\ell_4/\ell_1 = 1$  (dotted),  $\ell_4/\ell_1 = 2$  (dot-dashed) and  $\ell_4/\ell_1 = 4$  (dashed)

two multi-scale models. For this particular combination of parameters, the dispersion curves for various ratios of  $\ell_4/\ell_1$  are shown in Figure 1. As can be seen, the relevant values of the curve are the intercept and the horizontal asymptote, the numerical values of which follow from Eq. (21) through

$$\lim_{k \rightarrow 0} c = c_e \sqrt{1 + \frac{q^2}{\mu E}} \quad (24a)$$

$$\lim_{k \rightarrow \infty} c = c_e \sqrt{1 + \frac{q^2}{\mu E}} \cdot \frac{\ell_1}{\ell_4} \quad (24b)$$

Note that the case  $\ell_4/\ell_1 = 1$  is non-dispersive as  $c \neq c(k)$ .

Next, finite  $c_m$  will be assumed, which means the multi-scale model without **transient magnetic effects** will not be considered. As mentioned above, the difference between the mono-scale model of Eq. (19) and the multi-scale model with **transient magnetic effects** of Eq. (23) concerns the last term in each of these expressions. To verify the importance of this term, we will study the effect of  $\ell_2$  whilst taking the inertia length scales  $\ell_5 = \ell_4$  and the static length scales  $\ell_3 = \ell_1$ .

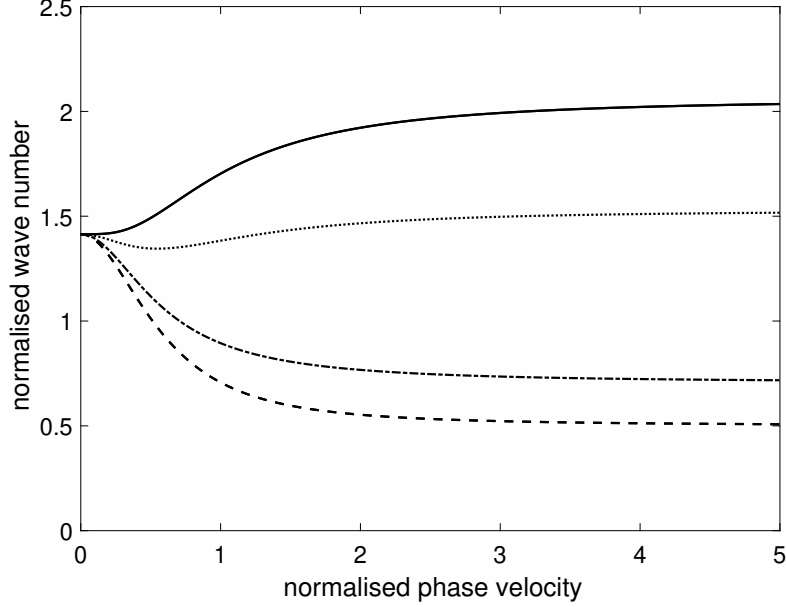


Figure 2: Normalised phase velocity  $c/c_e$  against normalised wave number  $\ell_1 k$  for finite  $c_m$ :  $\ell_2/\ell_1 = 2$  (solid),  $\ell_2/\ell_1 = 1.7$  (dotted),  $\ell_2/\ell_1 = 1$  (dot-dashed) and  $\ell_2/\ell_1 = 0$  (dashed)

With these simplifications, Eq. (19) can be resolved to give

$$c^2 = \frac{1 + \ell_1^2 k^2}{1 + \ell_4^2 k^2} \left( \frac{c_m^2 + c_e^2}{2} \pm \sqrt{\frac{(c_m^2 - c_e^2)^2}{4} - c_m^2 c_e^2 \cdot \frac{q^2}{\mu E} \cdot \frac{(1 + \ell_2^2 k^2)^2}{(1 + \ell_1^2 k^2)^2}} \right) \quad (25)$$

while the solution of Eq. (23) can be found by taking  $\ell_2 = \ell_1$ . Given the large discrepancy between  $c_m$  and  $c_e$ , the larger of the two solutions of Eq. (25) can be associated with the propagation of the magnetic waves, whereas the smaller one is related to the mechanical waves. The solutions have been evaluated numerically for  $q^2/\mu E = 1$  and  $c_m/c_e = 10^6$ . Furthermore, we have taken  $\ell_4/\ell_1 = 2$  and a number of values for  $\ell_2/\ell_1$ . Figure 2 shows the mechanical phase velocities. A first observation in comparing Figures 1 and 2 is that  $\ell_2$  and  $\ell_4$  have competing effects on the dispersion curves, which is in line with the mathematical structure of Eq. (19). The multi-scale model with **transient magnetic effects** is retrieved for  $\ell_2 = \ell_1$  and the corresponding curve is a scaled version of the one found in Figure 1. Interestingly, there is a small band of values for  $\ell_2$  for which the dispersion curve exhibits not one but two points of inflexion—here demonstrated for  $\ell_2/\ell_1 = 1.7$ . This is qualitative behaviour that is not captured by the multi-scale

model; thus, for such situations one needs to resort to the mono-scale model of Eqns. (2).

**Remark 3.** *The magnetic phase velocities according to the larger root of Eq. (25) did not show a noticeable difference between various values of  $\ell_2/\ell_1$  due to the large value of  $c_m/c_e$ . The resulting curves follow the monotonically decreasing trends shown in Figure 1 and have not been shown separately.*

**Remark 4.** *It remains to be seen whether the dispersion analysis is practically relevant for normalised wave numbers much larger than one, given that this bound typically coincides with the First Brillouin Zone. This would depend on the particular source and scale of microstructural heterogeneity. However, irrespective of this point we argue it is pertinent to verify the model behaviour for the larger wave numbers, because these may occur and be triggered in analytical and numerical implementations of the model where there may not be an upper limit on the resolution of the response. It is thus important to verify that anomalies, such as imaginery or unbounded phase velocities, do not occur.*

## 6. Concluding remarks

We have developed a number of models that extend earlier work on gradient-enriched piezomagnetic coupling from statics to dynamics. One mono-scale and two multi-scale formulations have been presented, whereby the multi-scale models either ignore or include **transient magnetic effects**. The mono-scale model consists of two coupled equations including fourth-order spatial derivatives, which makes implementation in standard finite element software cumbersome. The two multi-scale models consist of three or four coupled equations, but the highest order of spatial derivatives is second-order, hence implementation is straightforward.

The mono-scale model has five independent length scale parameters, whereas the multi-scale models include only two (in the absence of **transient magnetic effects**) or four (in the presence of **transient magnetic effects**). We have carried out an analysis of dispersive waves. The multi-scale models are able to capture the essential behaviour exhibited by the mono-scale model, with one exception that is observed for a small range of values of one of the length scales.

This study has an explorative character and is focussed on model formulation and a qualitative understanding of model behaviour. More quantitative investigations, including validation of length scale parameters, will be aided by studying a wider range of geometries in multiple dimensions. This can be achieved with

finite element simulations which may be based on the multi-scale formulations presented in this paper.

### **Acknowledgement**

The first author gratefully acknowledges financial support from the China Scholarship Council and the National Natural Science Foundation of China (Grant no. 11772045). The second and third authors gratefully acknowledge support of the EU RISE project FRAMED-734485.

### **References**

- [1] J.S. Stölken, A.G. Evans, A microbend test method for measuring the plasticity length scale, *Acta Mater.* 46 (1998) 5109–5115.
- [2] A.W. McFarland, J.S. Colton, Role of material microstructure in plate stiffness with relevance to microcantilever sensors, *J. Micromech. Microengng.* 15 (2005) 1060–1067.
- [3] D.C.C. Lam, F. Yang, A.C.M. Chong, J. Wang, P. Tong, Experiments and theory in strain gradient elasticity, *J. Mech. Phys. Solids* 51 (2003) 1477–1508.
- [4] A. Berezovski, J. Engelbrecht, M. Berezovski, Waves in microstructured solids: a unified viewpoint of modeling, *Acta Mech.* 220 (2011) 349–363.
- [5] S. Sidhardh, M.C. Ray, Dispersion curves for Rayleigh–Lamb waves in a micro-plate considering strain gradient elasticity, *Wave Motion* 86 (2019) 91–109.
- [6] I.V. Andrianov, J. Awrejcewicz, D. Weichert, Improved continuous models for discrete media, *Math. Probl. Engng.* 2010 (2010) 986242.
- [7] S. Gonella, M.S. Greene, W.K. Liu, Characterization of heterogeneous solids via wave methods in computational microelasticity, *J. Mech. Phys. Solids* 59 (2011) 959–974.
- [8] M.A. Eltaher, M.E. Khater, S.A. Emam, A review on nonlocal elastic models for bending, buckling, vibrations, and wave propagation of nanoscale beams, *Appl. Math. Model.* 40 (2016) 4109–4128.

- [9] B. Arash, Q. Wang, A review on the application of nonlocal elastic models in modeling of carbon nanotubes and graphenes, *Comput. Mater. Sci.* 188 (2014) 57–82.
- [10] V.A. Eremeyev, L.P. Lebedev, M.J. Cloud, Acceleration waves in the nonlinear micromorphic continuum, *Mech. Res. Comm.* 93 (2018) 70–74.
- [11] W. Xiao, L. Li, M. Wang, Propagation of in-plane wave in viscoelastic monolayer graphene via nonlocal strain gradient theory, *Appl. Phys. A* 123 (2017) 1–9.
- [12] A. Madeo, P. Neff, I.D. Ghiba, G. Rosi, Reflection and transmission of elastic waves in non-local band-gap metamaterials: A comprehensive study via the relaxed micromorphic model, *J. Mech. Phys. Solids* 95 (2016) 441–479.
- [13] K. Tamm, T. Peets, J. Engelbrecht, D. Kartofelev, Negative group velocity in solids, *Wave Motion* 71 (2017) 127–138.
- [14] N. Auffray, J. Dirrenberger, G. Rosi, A complete description of bi-dimensional anisotropic strain-gradient elasticity, *Int. J. Solids Struct.* 69–70 (2015) 195–206.
- [15] N. Auffray, Q.C. He, H. Le Quang, Complete symmetry classification and compact matrix representations for 3D strain gradient elasticity, *Int. J. Solids Struct.* 159 (2019) 197–210.
- [16] R. Hu, C. Oskay, Spatial–temporal nonlocal homogenization model for transient anti-plane shear wave propagation in periodic viscoelastic composites, *Comput. Methods Appl. Mech. Engng.* 342 (2018) 1–31.
- [17] R. Hu, C. Oskay, Multiscale nonlocal effective medium model for in-plane elastic wave dispersion and attenuation in periodic composites, *J. Mech. Phys. Solids* 124 (2019) 220–243.
- [18] D. De Domenico, H. Askes, A new multi-scale dispersive gradient elasticity model with microinertia: Formulation and  $C^0$ -finite element implementation, *Int. J. Numer. Methods Engng* 108 (2016) 485–512.
- [19] D. De Domenico, H. Askes, Nano-scale wave dispersion beyond the first brillouin zone simulated with inertia gradient continua, *J. Appl. Phys.* 124 (2018) 205107.

- [20] G. Rosi, L. Placidi, N. Auffray, On the validity range of strain-gradient elasticity: A mixed static-dynamic identification procedure, *Eur. J. Mech. A/Solids* 69 (2018) 179—191.
- [21] R. Hu, C. Oskay, Nonlocal homogenization model for wave dispersion and attenuation in elastic and viscoelastic periodic layered media, *J. Appl. Mech.* 84 (2017) 031003.
- [22] D. De Domenico, H. Askes, E.C. Aifantis, Gradient elasticity and dispersive wave propagation: Model motivation and length scale identification procedures in concrete and composite laminates, *Int. J. Solids Struct.* 158 (2019) 176—190.
- [23] H. Askes, E.C. Aifantis, Gradient elasticity in statics and dynamics: An overview of formulations, length scale identification procedures, finite element implementations and new results, *Int. J. Solids Struct.* 48 (2011) 1962—1990.
- [24] R.D. Mindlin, Micro-structure in linear elasticity, *Arch. Ration. Mech. Anal.* 16 (1964) 51–78.
- [25] K.B. Mustapha, D. Ruan, Size-dependent axial dynamics of magnetically-sensitive strain gradient microbars with end attachments, *Int. J. Mech. Sci.* 94–95 (2015) 96–110.
- [26] A.C. Eringen, On differential equations of nonlocal elasticity and solutions of screw dislocation and surface waves, *J. Appl. Phys.* 54 (1983) 4703–4710.
- [27] U. Güven, Transverse vibrations of single-walled carbon nanotubes with initial stress under magnetic field, *Compos. Struct.* 114 (2014) 92–98.
- [28] F. Ebrahimi, M.R. Barati, Through-the-length temperature distribution effects on thermal vibration analysis of nonlocal strain-gradient axially graded nanobeams subjected to nonuniform magnetic field, *J. Therm. Stress* 40 (2017) 548–563.
- [29] F. Ebrahimi, M.R. Barati, Vibration analysis of graphene sheets resting on the orthotropic elastic medium subjected to hygro-thermal and in-plane magnetic fields based on the nonlocal strain gradient theory, *Proc. Inst. Mech. Engrs. C: J. Mech. Engng. Sci.* 232 (2017) 1–13.

- [30] B. Karami, D. Shahsavari, M. Janghorban, Wave propagation analysis in functionally graded (FG) nanoplates under in-plane magnetic field based on nonlocal strain gradient theory and four variable refined plate theory, *Mech. Adv. Mater. Struct.* 25 (2017) 1–11.
- [31] F. Ebrahimi, M.R. Barati, Flexural wave propagation analysis of embedded S-FGM nanobeams under longitudinal magnetic field based on nonlocal strain gradient theory, *Arab. J. Sci. Engng.* 42 (2017) 1715–1726.
- [32] E. Farno, J.C. Baudez, N. Eshtiaghi, Comparison between classical Kelvin-Voigt and fractional derivative Kelvin-Voigt models in prediction of linear viscoelastic behaviour of waste activated sludge, *Sci. Total Environ.* 613–614 (2018) 1031–1036.
- [33] A. Ghorbanpour Arani, M. Shokravi, Vibration response of visco-elastically coupled double-layered visco-elastic graphene sheet systems subjected to magnetic field via strain gradient theory considering surface stress effects, *Proc. Inst. Mech. Engrs. N: J. Nanomater. Nanoengng. Nanosyst.* 229 (2015) 180–190.
- [34] L. Li, Y. Hu, L. Ling, Wave propagation in viscoelastic single-walled carbon nanotubes with surface effect under magnetic field based on nonlocal strain gradient theory, *Physica E: Low-Dim. Syst. Nanostruct.* 75 (2015) 118–124.
- [35] S. Chikazumi, *Physics of Ferromagnetism*, Oxford Univ. Press, 1997.
- [36] R. Gholami, R. Ansari, Y. Gholami, Size-dependent bending, buckling and vibration of higher-order shear deformable magneto-electro-thermo-elastic rectangular nanoplates, *Mater. Res. Express* 4 (2017) 065702.
- [37] L.L. Ke, Y.S. Wang, J. Yang, S. Kitipornchai, The size-dependent vibration of embedded magneto-electro-elastic cylindrical nanoshells, *Smart Mater. Struct.* 23 (2014) 125036.
- [38] L.L. Ke, Y.S. Wang, J. Yang, S. Kitipornchai, Free vibration of size-dependent magneto-electro-elastic nanoplates based on the nonlocal theory, *Acta Mech. Sin.* 30 (2014) 516–525.
- [39] S. Sahmani, M.M. Aghdam, Nonlocal strain gradient shell model for axial buckling and postbuckling analysis of magneto-electro-elastic composite nanoshells, *Compos. B Engng.* 132 (2018) 258–274.

- [40] L.H. Ma, L.L. Ke, J.N. Reddy, J. Yang, S. Kitipornchai, Y.S. Wang, Wave propagation characteristics in magneto-electro-elastic nanoshells using non-local strain gradient theory, *Compos. Struct.* 199 (2018) 10—23.
- [41] F. Ebrahimi, A. Dabbagh, On flexural wave propagation responses of smart FG magneto-electro-elastic nanoplates via nonlocal strain gradient theory, *Compos. Struct.* 162 (2017) 281—293.
- [42] F. Ebrahimi, A. Dabbagh, Nonlocal strain gradient based wave dispersion behavior of smart rotating magneto-electro-elastic nanoplates, *Mater. Res. Express* 4 (2017) 025003.
- [43] F. Ebrahimi, A. Dabbagh, Wave dispersion characteristics of rotating heterogeneous magneto-electro-elastic nanobeams based on nonlocal strain gradient elasticity theory, *J. Electromagn. Waves Appl.* 32 (2018) 138—169.
- [44] Y.M. Yue, K.Y. Xu, E.C. Aifantis, Microscale size effects on the electromechanical coupling in piezoelectric material for anti-plane problem, *Smart Mater. Struct.* 23 (2014) 125043.
- [45] M. Xu, I.M. Gitman, H. Askes, A gradient-enriched continuum model for magneto-elastic coupling: Formulation, finite element implementation and in-plane problems, *Comput. Struct.* 212 (2019) 275–288.
- [46] H. Askes, T. Bennett, E.C. Aifantis, A new formulation and  $C^0$ -implementation of dynamically consistent gradient elasticity, *Int. J. Numer. Methods Engng.* 72 (2007) 111–126.
- [47] T. Bennett, I.M. Gitman, H. Askes, Elasticity theories with higher-order gradients of inertia and stiffness for the modelling of wave dispersion in laminates, *Int. J. Fracture* 148 (2007) 185–193.
- [48] T. Bennett, H. Askes, Finite element modelling of wave dispersion with dynamically consistent gradient elasticity, *Comput. Mech.* 43 (2009) 815–825.